Published in final edited form as:
Toxicol Appl Pharmacol. 2013 October 1; 272(1): 86–95. doi:10.1016/j.taap.2013.05.020.

Tissue factor pathway inhibitor prevents airway obstruction, respiratory failure and death due to sulfur mustard analog inhalation

Raymond C. Rancourt[1], **Livia A. Veress**[1], **Aftab Ahmad**[1], **Tara B. Hendry-Hofer**[1], **Jacqueline S. Rioux**[1], **Rhonda B. Garlick**[1], and **Carl W. White**[1]

Livia A. Veress: livia.veress@ucdenver.edu; Aftab Ahmad: aftab.ahmad@ucdenver.edu; Tara B. Hendry-Hofer: tara.hendry-hofer@ucdenver.edu; Jacqueline S. Rioux: jacqueline.rioux@ucdenver.edu; Rhonda B. Garlick: rhonda.garlick@ucdenver.edu; Carl W. White: carl.w.white@ucdenver.edu

[1]Department of Pediatrics, University of Colorado, Denver CO

Abstract

Sulfur mustard (SM) inhalation causes airway injury, with enhanced vascular permeability, coagulation, and airway obstruction. The objective of this study was to determine whether recombinant tissue factor pathway inhibitor (TFPI) could inhibit this pathogenic sequence.

Methods—Rats were exposed to the SM analog 2-chloroethyl ethyl sulfide (CEES) via nose-only aerosol inhalation. One hour later, TFPI (1.5 mg/kg) in vehicle, or vehicle alone, were instilled into the trachea. Arterial O_2 saturation was monitored using pulse oximetry. Twelve hours after exposure, animals were euthanized and bronchoalveolar lavage fluid (BALF) and plasma analyzed for prothrombin, thrombin-antithrombin complex (TAT), active plasminogen activator inhibitor-1 (PAI-1) levels, and fluid fibrinolytic capacity. Lung steady-state PAI-1 mRNA was measured by RT-PCR analysis. Airway-capillary leak was estimated by BALF protein and IgM, and by pleural fluid measurement. In additional animals, airway cast formation was assessed by microdissection and immunohistochemical detection of airway fibrin.

Results—Airway obstruction in the form of fibrin-containing casts were evident in central conducting airways of rats receiving CEES. TFPI decreased cast formation, and limited severe hypoxemia. Findings of reduced prothrombin consumption, and lower TAT complexes in BALF, demonstrated that TFPI acted to limit thrombin activation in airways. TFPI, however, did not appreciably affect CEES-induced airway protein leak, PAI-1 mRNA induction, or inhibition of the fibrinolytic activity present in airway surface liquid.

Conclusions—Intratracheal administration of TFPI limits airway obstruction, improves gas exchange, and prevents mortality in rats with sulfur mustard-analog-induced acute lung injury.

Address correspondence to: Raymond C. Rancourt, Pediatric Airway Research Center, University of Colorado, 12700 E. 19th Ave mailstop 8615 Room P15-4020, Aurora, CO 80045, Ph: (303) 724-4654, Fax: (303) 724-7334, raymond.rancourt@ucdenver.edu.

Authors declare no competing interests, financial or otherwise.

Contribution: R.C.R., A.A., T.B.H., L.A.V., R.B.G. and J.R. performed experiments; R.C.R. analyzed results and made figures; R.C.R designed the experiments; R.C.R. and C.W.W. wrote the paper.

Keywords

Sulfur mustard; inhalation; lung injury; TFPI; airway; coagulation

Introduction

Sulfur mustard (SM), commonly known as mustard gas, is a chemical weapon deployed in several 20th century military conflicts. Casualties from SM likely exceed the combined sum caused by all other chemical weapons (Szinicz, 2005). It remains a threat due to its ease of manufacture, potential for causing mass casualties, and existence of large stockpiles. SM poisoning damages the eyes, skin, with respiratory failure being the principle cause of mortality (Papirmeister, 1991). The laryngeal and tracheobronchial airway epithelia are especially susceptible to injury. Following inhalation, the victim is asymptomatic for 2-12 hours. Symptoms include pain, cough, progressive rhinosinusitis and tracheobronchitis, with hemorrhagic pulmonary edema and respiratory failure within 20-48 hours, depending on dose inhaled (Winternitz, 1919; Hosseini *et al.*, 1989; Somani and Babu, 1989).

SM's vesicant properties are due to an intermolecular chemical reaction, forming a highly reactive electrophile. The nucleophilic central sulfur atom reacts with an electrophilic terminal carbon atom, displacing chlorine. The product, the sulphonium ion, is capable of alkylating DNA, protein, and lipid membranes (Herriott *et al.*, 1946; Lawley and Brookes, 1965). A similar reaction by the second terminal chlorine of SM enables a second alkylating reaction. CEES is a mustard analog lacking the second chlorine at the terminal 4-carbon position. Thus, CEES is only capable of monofunctional alkylating reactions. Nonetheless, CEES is capable of DNA and protein alkylation (Mozier and Hoffman, 1990); and retains the vesicant properties of SM (Gautum *et al.*, 2006). Lower toxicity along with commercial availability allow for CEES to be used as a model for SM in most laboratory settings.

Excessive fibrin deposition can elicit respiratory dysfunction and airway obstruction during acute lung injury (ALI) from chemical or microbial insult (Idell, 2003). Initial increased permeability of lung vasculature allows influx of fibrinogen and coagulation factors to the airway (Veress *et al.*, 2010). Extravascular tissue factor (TF) expression then initiates clotting at sites of injury or infection by activating Factor VII to Factor VIIa, inducing proteolytic activation of Factor X (FX) to FXa (Idell *et al.*, 1988; Idell *et al.*, 1989). Inhibition of TF has previously been shown to attenuate fibrin deposition in animal models of lung sepsis and pneumonia (Creasey *et al.*, 1993; Welty-Wolf *et al.*, 2001; Van Den Boogaard *et al.*, 2011). In addition to TF-dependent clot initiation, ALI also promotes airway fibrin deposition by suppressing fibrinolytic activity. Induction of plasminogen activator inhibitor-1 (PAI-1) is believed to be the principal mechanism for limiting fibrinolysis. (Bertozzi *et al.*, 1990).

Previously we demonstrated that in vitro application of TFPI was effective in limiting the elevated procoagulant activity of BALF recovered after CEES-induced lung injury (Rancourt *et al.*, 2012). In this study we used a rat model of CEES inhalation to determine if obstruction and resulting respiratory complications could be prevented by administration of TFPI directly to the airway. After establishing airway pharmacokinetics, we determined whether TFPI reduces airway cast formation and improves tissue oxygenation. We also examined processes by which TFPI affects lung coagulation including thrombin activation, PAI-1 expression and its impact on the fibrinolytic activity of BALF.

Methods

Reagents

Tifacogin (Novartis; Basel, Switzerland), produced in E coli, is a recombinant form of endogenous TFPI. SDS-PAGE and coomassie staining of non-reduced Tifacogin preparations revealed a single protein migrating at ~30 kDa and the absence of inclusion bodies (data not shown).

Animals and CEES Exposure Protocol

Male Sprague-Dawley rats (250-300 g; Harlan (Indianapolis, IN) were acclimated to Denver altitude for 1 week with ad libitum food and water. Prior to exposure, rats received an intraperitoneal injection of ketamine (50 mg/kg), xylazine (5 mg/kg) and acepromazine (1 mg/kg). After anesthesia, rats were loaded into polycarbonate tubes in a Jaeger nose-only inhalation system (CH Technologies, Westwood, NJ, USA). Dry air (6 L/min) was mixed with additional compressed air (6 L/min) containing ethanolic CEES (90% ethanol:10% CEES;v:v) and delivered to a bioaerosol nebulizing generator (BANG) via syringe pump. (Razel Scientific, St. Albans, VT). After 15 min exposure, BANG was terminated, and rats returned to cages. Control rats were exposed in identical fashion to diluent (100% ethanol). For rescue therapy, rats were anesthetized using isoflurane, and the trachea visualized by fiber optic laryngoscopy. An aerosolizer (Model IA-1C; Penn-Century, Inc., Philadelphia, PA,) was then inserted past the vocal cords, and 50 μl of vehicle (300 mM L-arginine, 20 mM sodium citrate, pH 5.5) or tifacogin (1.5 mg/kg) aerosolized into airways at 1, 3 and 5 hours after CEES.

Measurement of TFPI concentration and activity in BALF

BALF was analyzed for extracellular TFPI by use of an imubind total TFPI ELISA system (American Diagnostica, Stamford, CT). Rat TFPI is not recognized by this assay. TFPI activity was assayed by measuring inhibition of FXa-dependent substrate cleavage. Ten μl of BALF was incubated in a 96-well plate for 45 min at 37°C with 35 μl of HBSA buffer (137 mM NaCl, 5.38 mM KCl, 5.55 mM glucose, 10 mM HEPES, 0.1% BSA; pH 7.4), 5 μl of 1× innovin, and 50 μl of HBSA containing 50 nM FVII, 35 nM FX, and 12 mM $CaCl_2$. After incubation, 25 μl of 25 mM EDTA was added terminating FXa generation. Twenty five μl of S-2765 FXa substrate (6 mM; Chromogenix; Bedford, MA) was added to each well and absorbance at 405 nm was recorded after 60 seconds. FXa activity was expressed as a percentage of the absorbance reached by control samples having PBS substituted for BALF (100% activity).

Pulse oximetry

Oxygen saturation was monitored using the MouseOx oximeter (Starr Life Science, Pittsburgh, PA). The large rat (300 g) sensor collar was used. Three measurements per time point were taken.

Fibrin immunohistochemistry

Paraffin-embedded tissues were sectioned at 5 μm thickness and immunostained using a peroxidase-based Envision detection system (DAKO; Carpinteria, CA). Primary antibody for fibrin(ogen) was polyclonal rabbit anti-human fibrinogen (DAKO), at 1:3000 concentration for 60-minutes. Rabbit IgG control (DAKO) was used at the same specifications. The counterstaining was hematoxylin.

Microdissection and airway cast scoring

Cast scoring was done via microdissection as previously described by our group (Veress *et al,* 2010; Veress *et al,* 2013). Fixed lung was separated into five individual lobes by cross-sectioning each lobar bronchus at the site of immediate takeoff from the central airway bronchus. To obtain the "main airway cast score", each lobe was positioned separately onto a petri-dish, with its main lobar bronchus facing perpendicular to the microdissecting scope lens. Gravity dependent major daughter airways are the most cast-occluded in this model, thus we assessed each lobar major (largest) gravity-dependent airway for occlusion separately. To obtain "dependent airway" cast score, microdissection was performed to the level of the first gravity dependent (ventrally directed) major airway daughter branch. The dependent branch was then cross-sectioned at its immediate take off position and aligned in a perpendicular manner under the dissecting scope. A digital picture (by Olympus C-750 camera, Olympus Imaging America, Inc.) was then obtained of each main and dependent lobar opening, inclusive of casts within the airway, if present. Image-J (1.44p, NIH, USA) software was used to assess percent airway occlusion due to the cast (# of pixels of cast within the airway, divided by # of pixels of entire airway area, multiplied by 100). To obtain a quantitative score that can be used to assess drug therapy effects, the percent occlusion for each lobar main bronchus was then converted to a nominal score, based on a scale of 0 to 7 (0=0-4%, 1=5-14%, 2=15-29%, 3=30-49%, 4=50-64%, 5=65-79%, 6=80-99%, 7=100% occluded). Each lobar nominal cast score was then weighted based on volumetric differences of rat lobes to total lung (Zeltner *et al,* 1990) (raw score was multiplied by % of lobar volume as to the whole/100). This was calculated for each main and dependent score separately. The five separate lobe's weighted scores were then added together to obtain the "main" or "dependent" composite cast score for that particular animal (total score of 0 to 7). All personnel were blinded as to the specimen's identity and its treatment group throughout the procedure.

Prothrombin western analysis

BALF samples were centrifuged (800 g) and volumes containing 15 μg of total protein added to 5× Laemmli buffer and loaded onto 4-15% gradient SDS-polyacrylamide gels. After transfer, membranes were initially stained with Ponceau S, blocked for 1 hr in PBS containing 5% milk, followed by overnight incubation with a rabbit polyclonal Ab to thrombin (Abcam ab883981, Cambridge, MA). Blots were washed in Tris-buffered saline with 0.5% Tween 20 for 1 hr followed by incubation with a goat anti-rabbit secondary(1:7,000; Southern Biotechnology, Birmingham, AL). The rat prothrombin standard was from Molecular Innovations (Novi, MI).

IgM and Total Protein Measurement in Bronchoalveolar Lavage Fluid

IgM measured in BALF using standard ELISA (Bethyl Laboratories, Inc., Montgomery, TX). Total protein measured using bicinchoninic acid (BCA) protein assay (Pierce, Rockville, IL). Pleural fluid was collected from the pleural cavity of rats by insertion of 5-ml syringe affixed with rubber tubing.

Measurement of TAT complex, PAI-1 protein and mRNA measurements

TAT complex and PAI-1 were measured in BALF or plasma using an Enzygnost TAT microassay (Siemens; Tarrytown, NY), or rat PAI-1 active assay kit (Molecular Innovations; Novi, MI). For TAT measurement, plasma was diluted 1:1 in 0.9% saline. For mRNA measurement, total RNA was isolated by RNeasy mini system (Qiagen; Valencia, CA) using entire left lung lobe 12 hr after exposure. Next, cDNA was synthesized using Taqman reverse transcriptase kit (Applied Biosystems; Foster City CA) followed by real time PCR

using Taqman probes and normalization of data to 18S rRNA. Rat PAI-1 probe sequences were:

FAM-CGTTCACCAGCACCAGGCGT-TAMRA

Primer-L: GAGGCACACCAAAGGTATGA

Primer-R: ATTGGCCGTTGAAATAGAGG

Fibrinolytic assay

One ml of 25 mM phosphate buffer (pH 7.5) containing fibrinogen (3 mg/ml) was added to plates (12 well) containing 40 μl of bovine thrombin (200 NIH units/ml). After overnight solidification at 37°C, BALF supernatant (25 μl) was added to the fibrin matrix surfaces, incubated (12 hr), stained with 20% methanol containing amido black (10 mg/ml), and rinsed 3×. Plates were scanned using imageJ software (NIH) to determine area of fibrin clearance.

Plasma Isolation & Clotting Time Measurements

Rat blood was collected from inferior vena cava into 5-ml syringes containing 3.2% sodium citrate (citrate:blood = 1:9 v:v). After centrifugation, the upper ¾ of plasma was removed and frozen at −80°C. Clotting time was measured on recalcified plasma by adding into a 96-well plate: 50 μL of plasma diluted 1:1 in saline & 100 μL of saline. The clotting reaction was then initiated by adding 50 μL of 30 mM $CaCl_2$. Absorbance values at 405 nm were measured at 20-s intervals for 12 min in a SpectraMax 340 plate reader (37°C). A well was considered clotted at the first time point when absorbance reached within 0.003 units of the maximal value during the 12-min run.

Statistics

Statistical analyses utilized Prism 4 software. Means were compared by one-way analysis of variance followed by Tukey's test. Survival curves were compared by Kaplan-Meier log-rank test (Mantel-Cox). *P* values < 0.05 considered significant.

Results

Pharmacokinetics of tifacogin (TFPI) administration

A single bolus of 1.5 mg/kg of TFPI was delivered into the trachea to assess clearance. After delivery, BAL was performed at 0, 1, 2, or 4 hours and concentration determined by ELISA. Immediately after instillation, peak levels (0 hr) of TFPI were 8.71 ± 1.39 μg/ml (Figure 1A). After peak, there was a time-dependent decline in recoverable TFPI from BALF (1 hr: 3.85 ± 0.83 μg/ml; 2 hr: 2.82 ± 0.75 μg/ml; 4 hr: 1.13 ± 0.41 μg/ml). On the basis of the 2 and 4 hr timepoint concentrations, TFPI half-life in airways was 91 minutes. TFPI in BALF was also tested for capacity to inhibit generation of FXa by FVIIa/tissue factor catalytic complex (Figure 1B). Reactions in which naïve BALF was added had a mean absorbance value of 0.299 +/− .015, which did not significantly differ from control reactions conducted in the absence of BALF: 0.303 +/− 0.006. In contrast, BALF from TFPI-treated rats showed a time-dependent inhibition of FX activity (0 hr: 0.028 ± 0.017; 1 hr: 0.057 ± 0.033; 2 hr: 0.149 ± 0.059; 4 hr: 0.235 ± 0.035). This demonstrated functional TFPI retention in airways several hours after administration.

CEES-induced hypoxemia and reversal by TFPI

This study (Figure 1C) was designed to determine whether TFPI administration to airways could limit coagulation and respiratory distress associated with mustard injury. Anesthetized

rats were given nose-only inhalation of an ethanolic solution containing CEES (90% ethanol; 10% CEES), followed by treatment with vehicle or TFPI (1, 3, and 5 hr). As shown in Figures 2A and 2B, rats demonstrated peripheral arterial oxygen (Sp_{O2}) levels above 90% prior to CEES inhalation. In rats administered CEES + vehicle, Sp_{O2} decreased below 90% at 4-5 hours after exposure. Arterial oxygen of these rats continued to decline over the next 8 hours. In contrast, Sp_{O2} levels of rats given TFPI did not decrease to the extent seen in the vehicle group. Additionally, whereas no rebound was observed after vehicle, oxygenation improved in TFPI-treated rats. At 6 hr (Figure 2C), only TFPI treatment significantly increased oxygenation relative to that seen in rats exposed to CEES only. At 12 hr (Figure 2D), mean Sp_{O2} remained significantly higher in TFPI-treated rats, with oxygenation now comparable to rats not exposed to CEES (ethanol control).

TFPI reduces CEES-induced fibrin cast formation

Fibrin-immunostaining was performed on lung sections from the left main and right accessory lobe bronchi obtained 12 hr after CEES exposure (Figure 3). Large airways from rats exposed to CEES alone or CEES + vehicle treatment contained extensive fibrin deposits. Lung sections obtained after CEES + TFPI displayed considerably less immunoreactivity.

To assess extent of airway occlusion due to fibrin, airway microdissection was performed. This approach involved microscopic inspection of airway lumens to determine degree of obstruction (Figure 4A). These measurements were used to calculate occluded and patent airway lumenal areas of main and dependent central airways of all lung lobes. Thus, a score of 7 indicated maximal (100%) occlusion. These studies revealed prominent cast formation in both main and dependent airways in animals exposed to CEES only or CEES + vehicle (Figure 4B & C). However, animals administered TFPI after CEES exposure had considerably less airway obstruction.

Effect of TFPI on prothrombin, and TAT complex levels in BALF in response to CEES

Conversion of prothrombin zymogen to active thrombin is the key proteolytic step in fibrin formation. Western blot analysis using rat BALF after CEES exposure confirmed the presence of prothrombin in airways (Figure 5A). Two independent Western blot analyses also revealed significantly elevated prothrombin levels in BALF from tifacogin-treated animals relative to vehicle-treated rats (Figure 5C). Furthermore, recoverable TAT complexes in BALF increased dramatically after CEES only, or CEES + vehicle treatment, but were significantly less with CEES + TFPI (Figure 5D). These findings indicated that TFPI limits airway coagulation by inhibiting upstream events required for prothrombin cleavage.

TFPI did not alter vascular-airway leak due to CEES

As previously reported, CEES inhalation caused vascular leak into airways (Veress *et al.*, 2010). We sought to determine if anticoagulant administration would increase such leak due to CEES injury. CEES-exposed rats had elevated protein and IgM in BALF compared to rats inhaling only ethanol (Figures 6A & 6B). However, a comparison between groups of rats administered CEES, CEES + vehicle, or CEES + TFPI, showed that these leak parameters did not increase as a consequence of TFPI treatment. Since pleural effusions also may form in rats during lung injury, fluid accumulation also was compared between vehicle- and tifacogin-treated rats after CEES, and this was not increased by TFPI (Figure 6C).

Impact of CEES and TFPI on lung PAI-1 levels and airway fibrinolytic activity

Compared to ethanol controls, PAI-1 mRNA was elevated in lung homogenates after CEES inhalation (Figure 7A). These increases were not significantly attenuated by TFPI treatment. ELISA measurements were also used to measure active PAI-1 protein in BALF (Figure 7B). After ethanol, active PAI-1 levels in BALF were 0.61 +/- 0.82 ng/ml. PAI-1 levels were significantly elevated (5.47 +/− 4.48 ng/ml) after CEES + vehicle treatment. In contrast, PAI-1 protein increases by CEES were reduced in the group receiving TFPI (1.61 +/− 0.66 ng/ml). To determine actual fibrinolytic capacity of these samples, 25 μl of centrifuged BALF was placed on a fibrin matrix and incubated (Figure 7C). BALF from ethanol-treated controls exhibited the largest fibrinolytic area (127 +/− 49.8 mm^2), while CEES + vehicle (9.6 +/− 4.2 mm^2) and CEES + TFPI (8.4 +/− 3.6 mm^2) treated animals demonstrated less fibrinolysis. There was no significant difference between the latter two groups, an indication that TFPI did not relieve the suppression of fibrinolysis by CEES (Figure 7D).

Effect of CEES and tifacogin on plasma clotting time, TAT complex, and PAI-1 levels

Plasma from animals receiving inhaled ethanol only exhibited a mean clotting time of 414 +/− 36.8 seconds (Fig 8A). In contrast, 10% CEES inhalation reduced clotting time to 272 +/− 26.1 seconds. Plasma from rats given intratracheal vehicle after CEES also exhibited accelerated clotting (307.5 +/− 52.3 seconds), while TFPI treatment (526 +/− 31.3 seconds) had an anticoagulant effect.

Consistent with clotting time findings, plasma levels of TAT complexes (Figure 8B) were 2.5 times higher in CEES-exposed rats (26.75 +/− 7.76 μg/L*)* compared to ethanol-exposed controls (9.38 +/− 0.7 μg/L), supporting the rationale that CEES inhalation induced systemic hypercoagulability. Intratracheal delivery of vehicle did not impact plasma TAT complex (20.98 +/− 7.9 μg/L). Levels of TAT complexes did, however, decline after tifacogin treatment (3.32 +/− 0.6 μg/L). PAI-1 levels (Figure 8C) in plasma exhibited a similar pattern. Levels in the ethanol group were low (1.71 +/− 0.7 ng/ml), elevated in response to CEES (22.67 +/− 13.76 ng/ml), or CEES + vehicle (23.19+/− 11.33 ng/ml), and attenuated by CEES + tifacogin (9.70 +/− 6.58 ng/ml). Thus, CEES inhalation had procoagulant effects in peripheral blood as well as airways, and TFPI counteracted both. In separate experiments (Figure 8D), intratracheal delivery of TFPI to ethanol-exposed control rats had only a slight impact on TAT complex (9.08 +/− 1.2 μg/L) formation compared to rats exposed to ethanol only (10.65 +/− 4.14 μg/L) or ethanol + vehicle (13.46 +/− 2.25 μg/L). These differences were not significant.

Effect of TFPI on rat survival after 10% CEES inhalation

As shown in Figure 9, subjects inhaling CEES had a 75% survival rate at 12 hours. For rats exposed to CEES and receiving vehicle only, the survival rate was comparable (79%). In rats given CEES + tifacogin, survival remained at 100% for the experimental duration. A comparison of survival curves using Mantel-Cox log-rank test indicated that TFPI significantly improves survival.

Discussion

Tissue Factor Pathway Inhibitor (TFPI) is a 276 amino acid glycoprotein with 3 distinct structural domains and an acidic N-terminus (Lwaleed and Bass, 2006). The first domain binds and inactivates the TF/FVIIa complex, while the second binds and inactivates FXa. The third domain's role is not fully understood, but it may facilitate binding with lipoproteins. By virtue of these interactions, TFPI is believed to be the only endogenous regulator of the TF-dependent pathway of coagulation. Levels are low during acute lung

injury (Bastarache *et al.*, 2008). Tifacogin differs from the native protein by its lack of glycosylation and amino terminal alanine (Gustafson *et al.*, 1994).

While plasma half-life of TFPI is estimated to be 60-120 minutes (Valentin *et al.*, 1991; Harenberg *et al.*, 1995), no data exists regarding its clearance from airways. Earlier work has demonstrated the susceptibility of blood-borne TFPI to oxidation, adding uncertainty as to the duration TFPI might remain functional in an airway environment (Ohkura *et al.*, 2004). In our initial studies, TFPI was detected at high level after single dose intratracheal delivery, and exhibited gradual decay over 1, 2, and 4 hr. Using these latter, non-peak intervals, tifacogin half-life in airway surface liquid was calculated as 91 minutes, similar to half-life estimates for TFPI in plasma. Use of an assay to measure TFPI-dependent FXa inhibition showed inhibitory activity to be commensurate with TFPI concentration, an indication that its anticoagulant capacity was maintained during airway retention.

Respiratory distress and arterial oxygen desaturation are typically seen in obstructive airway disorders, including sulfur mustard inhalation. In this study, TFPI limited obstruction of main bronchi and dependent segmental branches. Two lines of evidence supported this conclusion. First, immunohistochemistry on lung sections indicated that airways had considerably less obstruction by fibrin-staining material with tifacogin treatment. Second, microdissection experiments demonstrate that quantitative cast formation was less severe in these subjects. Results of pulse oximetry further indicated that elimination of occlusive airway casts by TFPI improved gas exchange and oxygen delivery. It should be noted that improvements in tissue oxygenation occurred despite persistence of vascular airway leak in TFPI-treated rats. This latter observation indicated that impaired gas exchange was not simply due to edematous leak, but instead resulted from coagulation and obstruction. Comparisons between TFPI and vehicle treatment groups after CEES exposure indicated a non-significant downward trend in BALF IgM and protein levels. Frequently, negative pulmonary edema develops as a consequence of inspiring against an obstructed airway. Therefore, one possibility is that TFPI, by preventing airway obstruction, is also limiting this secondary form of edema.

Early onset of airway hemorrhage and edema in animal models of SM and CEES imply severe disruption of the vascular airway barrier (McClintock *et al.*, 2006; Allon *et al.*, 2009). During vascular leakage, the coagulation system is rapidly activated, causing conversion of prothrombin to thrombin. Nascent clot formation proceeds when thrombin cleaves fibrinogen into insoluble fibrin. Thrombin is sequestered from plasma by one of two processes. It may become clot-bound after being adsorbed onto fibrin, or it may be inactivated (Kumar *et al.*, 1994). The latter occurs when antithrombin binds and neutralizes thrombin, resulting in formation of TAT complex. Due to these interactions, thrombin's half-life is short, and it is difficult to measure. A comparison of prothrombin levels in vehicle- and tifacogin-treated animals demonstrated higher levels in the latter group, suggesting lack of consumption due to TFPI action. Elevated TAT complexes observed in the vehicle group, relative to TFPI-treated rats, supported this concept. These findings reinforce that TFPI did not appreciably impact vascular leak or the subsequent egress of coagulation factors. Instead, it acted by limiting participation of these constituents in the clotting process.

PAI-1 is a key inhibitor of fibrinolysis. Levels are low in non-injured lung, but can exhibit a prolonged induction in response to injury (Zeerleder *et al.*, 2006). In ARDS, fibrinoytic activity of BALF is decreased due to PAI-1 expression (Schultz *et al.*, 2004). Like other serpins, PAI-1 is metastable, existing in several conformations, including active, latent, or proteinase-complexed (Cale and Lawrence, 2007). Active PAI-1 is the only conformation capable of inhibiting plasminogen activation. In the present study, CEES inhalation promoted PAI-1 mRNA expression in lung. This did not differ between experimental CEES-

exposed groups administered vehicle or TFPI. Our findings that chemical insult causes elevated mRNA expression are consistent with findings of others demonstrating increased PAI-1 transcription in lungs of patients with ARDS when compared to control subjects (Chapman and Stone, 1985; Carley *et al.*, 1992). CEES exposure also increased the active form of PAI-1 protein in BALF, an effect partially attenuated by TFPI administration. These findings prompted us to test actual fibrinolytic capability of BALF (Figure 7). These latter measurements demonstrated greatly reduced fibrinolytic activity in response to mustard inhalation, which is not corrected by TFPI. Thus, we concluded that tifacogin inhibited CEES-induced airway obstruction by preventing clot initiation, and not by restoration of fibrinolytic activity. We are uncertain as to why the lowering of active PAI-1 protein expression by tifacogin did not translate to enhanced fibrinolysis. Since PAI-1 in TFPI-treated rats remained elevated relative to rats not exposed to CEES, this level of PAI-1 may still be sufficient to counteract the plasmin-activator present (Grau *et al.*, 1997). PAI-1 expression has previously been shown to potentiate fibrotic disease states. Modest correction in PAI-1 activity by TFPI, therefore, might still have a beneficial effect during subacute lung repair (Idell *et al.*, 2002).

Besides causing airway coagulopathy, severe ALI also promotes thrombosis within the pulmonary vasculature (Greene, 1986). In the current model, observations of accelerated clotting times and increased TAT complexes in plasma suggest that intravascular coagulation might occur with exposure to 10% CEES. Our previous work has demonstrated that TF-dependent microparticles are predominantly responsible for the increased procoagulant activity of BALF after CEES exposure (Rancourt *et al.*, 2012). It is possible that a similar mechanism is also responsible for the accelerated clotting of plasma in response to CEES inhalation. Importantly, airway administration of TFPI normalized these intravascular changes. Our observation that TFPI treatment does not significantly reduce basal TAT complex levels in plasma derived from ethanol-exposed control rats suggests that the amount of drug entering the systemic circulation from the lung could be influenced by the degree of lung permeability or injury caused by CEES exposure.

The current study demonstrated that TFPI administration to rat airways can significantly reduce development of fibrin-containing casts, lesions responsible for airway obstruction after CEES inhalation. Our findings of reduced consumption of prothrombin and lower TAT complex formation in BALF supported the concept that inhibition of thrombin activation represents the likely mechanism by which TFPI limits cast formation. Consistent with these findings, rats given TFPI demonstrated improved tissue oxygenation, and mortality was prevented.

Acknowledgments

This research is supported by the CounterACT Program, NIH Office of the Director, and the NIEHS, Grant Number U54 ES015678.

References

Allon N, Amir A, Manisterski E, Rabinovitz I, Dachir S, Kadar T. Inhalation exposure to sulfur mustard in the guinea pig model: clinical, biochemical and histopathological characterization of respiratory injuries. Toxicol Appl Pharmacol. 2009; 241:154–162. [PubMed: 19682477]

Bastarache JA, Wang L, Wang Z, Albertine KH, Matthay MA, Ware LB. Intra-alveolar tissue factor pathway inhibitor is not sufficient to block tissue factor procoagulant activity. Am J Physiol Lung Cell Mol Physiol. 2008; 294:L874–881. [PubMed: 18310227]

Bertozzi P, Astedt B, Zenzius L, Lynch K, LeMaire F, Zapol W, Chapman HA Jr. Depressed bronchoalveolar urokinase activity in patients with adult respiratory distress syndrome. N Engl J Med. 1990; 322:890–897. [PubMed: 2314423]

Cale JM, Lawrence DA. Structure-function relationships of plasminogen activator inhibitor-1 and its potential as a therapeutic agent. Curr Drug Targets. 2007; 8:971–981. [PubMed: 17896949]

Carley WW, Niedbala MJ, Gerritsen ME. Isolation, cultivation, and partial characterization of microvascular endothelium derived from human lung. Am J Respir Cell Mol Biol. 1992; 7:620–630. [PubMed: 1333246]

Chapman HA Jr, Stone OL. A fibrinolytic inhibitor of human alveolar macrophages. Induction with endotoxin. Am Rev Respir Dis. 1985; 132:569–575. [PubMed: 3898943]

Creasey AA, Chang AC, Feigen L, Wun TC, Taylor FB Jr, Hinshaw LB. Tissue factor pathway inhibitor reduces mortality from Escherichia coli septic shock. J Clin Invest. 1993; 91:2850–2860. [PubMed: 8514893]

Gautum A, Vijayaraghavan R, Sharma M, Ganesan K. Comparative toxicity studies of sulfur mustard (2,2′-dichloro diethyl sulfide) and monofunctional sulfur mustard (2-chloroethyl ethyl sulfide), administered through various routes in mice. J Med CBR Def. 2006; 4:1–21.

Grau GE, de Moerloose P, Bulla O, Lou J, Lei Z, Reber G, Mili N, Ricou B, Morel DR, Suter PM. Haemostatic properties of human pulmonary and cerebral microvascular endothelial cells. Thromb Haemost. 1997; 77:585–590. [PubMed: 9066014]

Greene R. Pulmonary vascular obstruction in the adult respiratory distress syndrome. J Thorac Imaging. 1986; 1:31–38. [PubMed: 3298679]

Gustafson ME, Junger KD, Wun TC, Foy BA, Diaz-Collier JA, Welsch DJ, Obukowicz MG, Bishop BF, Bild GS, Leimgruber RM, et al. Renaturation and purification of human tissue factor pathway inhibitor expressed in recombinant E. coli. Protein Expr Purif. 1994; 5:233–241. [PubMed: 7950366]

Harenberg J, Malsch R, Heene DL. Tissue factor pathway inhibitor: proposed heparin recognition region. Blood Coagul Fibrinolysis. 1995; 6(1):S50–56. [PubMed: 7647222]

Herriott RM, Anson ML, Northrop JH. Reaction of enzymes and proteins with mustard gas (BIS(beta-Chloroethyl)Sulfide. J Gen Physiol. 1946; 30:185–210. [PubMed: 19873486]

Hosseini K, Moradi A, Mansouri A, Vessal K. Pulmonary manifestations of mustard gas injury: a review of 61 cases. Ir J Med Sci. 1989; 14:20–26.

Idell S. Coagulation, fibrinolysis, and fibrin deposition in acute lung injury. Crit Care Med. 2003; 31:S213–220. [PubMed: 12682443]

Idell S, Mazar A, Cines D, Kuo A, Parry G, Gawlak S, Juarez J, Koenig K, Azghani A, Hadden W, McLarty J, Miller E. Single-chain urokinase alone or complexed to its receptor in tetracycline-induced pleuritis in rabbits. Am J Respir Crit Care Med. 2002; 166:920–926. [PubMed: 12359647]

Idell S, Peters J, James KK, Fair DS, Coalson JJ. Local abnormalities of coagulation and fibrinolytic pathways that promote alveolar fibrin deposition in the lungs of baboons with diffuse alveolar damage. J Clin Invest. 1989; 84:181–193. [PubMed: 2738151]

Idell S, Peterson BT, Gonzalez KK, Gray LD, Bach R, McLarty J, Fair DS. Local abnormalities of coagulation and fibrinolysis and alveolar fibrin deposition in sheep with oleic acid-induced lung injury. Am Rev Respir Dis. 1988; 138:1282–1294. [PubMed: 3202484]

Kumar R, Beguin S, Hemker HC. The influence of fibrinogen and fibrin on thrombin generation--evidence for feedback activation of the clotting system by clot bound thrombin. Thromb Haemost. 1994; 72:713–721. [PubMed: 7900079]

Lawley PD, Brookes P. Molecular mechanism of the cytotoxic action of difunctional alkylating agents and of resistance to this action. Nature. 1965; 206:480–483. [PubMed: 5319105]

Lwaleed BA, Bass PS. Tissue factor pathway inhibitor: structure, biology and involvement in disease. J Pathol. 2006; 208:327–339. [PubMed: 16261634]

McClintock SD, Hoesel LM, Das SK, Till GO, Neff T, Kunkel RG, Smith MG, Ward PA. Attenuation of half sulfur mustard gas-induced acute lung injury in rats. J Appl Toxicol. 2006; 26:126–131. [PubMed: 16252256]

Mozier NM, Hoffman JL. Biosynthesis and urinary excretion of methyl sulfonium derivatives of the sulfur mustard analog, 2-chloroethyl ethyl sulfide, and other thioethers. FASEB J. 1990; 4:3329–3333. [PubMed: 2253846]

Ohkura N, Hiraishi S, Itabe H, Hamuro T, Kamikubo Y, Takano T, Matsuda J, Horie S. Oxidized phospholipids in oxidized low-density lipoprotein reduce the activity of tissue factor pathway

inhibitor through association with its carboxy-terminal region. Antioxid Redox Signal. 2004; 6:705–712. [PubMed: 15242551]

Papirmeister, B. Medical defense against mustard gas: toxic mechanisms and pharmacological implications. CRC Press; Boca Raton: 1991.

Rancourt RC, Veress LA, Guo X, Jones TN, Hendry-Hofer TB, White CW. Airway tissue factor-dependent coagulation activity in response to sulfur mustard analog 2-chloroethyl ethyl sulfide. Am J Physiol Lung Cell Mol Physiol. 2012; 302:L82–92. [PubMed: 21964405]

Schultz MJ, Millo J, Levi M, Hack CE, Weverling GJ, Garrard CS, van der Poll T. Local activation of coagulation and inhibition of fibrinolysis in the lung during ventilator associated pneumonia. Thorax. 2004; 59:130–135. [PubMed: 14760153]

Somani SM, Babu SR. Toxicodynamics of sulfur mustard. Int J Clin Pharmacol Ther Toxicol. 1989; 27:419–435. [PubMed: 2681003]

Szinicz L. History of chemical and biological warfare agents. Toxicology. 2005; 214:167–181. [PubMed: 16111798]

Valentin S, Ostergaard P, Kristensen H, Nordfang O. Simultaneous presence of tissue factor pathway inhibitor (TFPI) and low molecular weight heparin has a synergistic effect in different coagulation assays. Blood Coagul Fibrinolysis. 1991; 2:629–635. [PubMed: 1664252]

Van Den Boogaard FE, Brands X, Schultz MJ, Levi M, Roelofs JJ, Van 't Veer C, Van Der Poll T. Recombinant human tissue factor pathway inhibitor exerts anticoagulant, anti-inflammatory and antimicrobial effects in murine pneumococcal pneumonia. Journal of thrombosis and haemostasis: JTH. 2011; 9:122–132. [PubMed: 21029363]

Veress LA, Hendry-Hofer TB, Loader JE, Rioux JS, Garlick RB, White CW. Tissue plasminogen activator prevents mortality from sulfur mustard analog-induced airway obstruction. Am J Respir Cell Mol Biol. 2013; 48:439–447. [PubMed: 23258228]

Veress LA, O'Neill HC, Hendry-Hofer TB, Loader JE, Rancourt RC, White CW. Airway obstruction due to bronchial vascular injury after sulfur mustard analog inhalation. Am J Respir Crit Care Med. 2010; 182:1352–1361. [PubMed: 20639443]

Welty-Wolf KE, Carraway MS, Idell S, Ortel TL, Ezban M, Piantadosi CA. Tissue factor in experimental acute lung injury. Seminars in hematology. 2001; 38:35–38. [PubMed: 11735108]

Winternitz MC. Anatomical changes in the respiratory tract initiated by irritating gases. Military Surgeon. 1919; 44:476–493.

Zeerleder S, Schroeder V, Hack CE, Kohler HP, Wuillemin WA. TAFI and PAI-1 levels in human sepsis. Thromb Res. 2006; 118:205–212. [PubMed: 16009400]

Zeltner TB, Bertacchini M, Messerli A, Burri PH. Morphometric estimation of regional differences in the rat lung. Experimental lung research. 1990; 16:145–158. [PubMed: 2328712]

Abbreviations

ALI	acute lung injury
BALF	bronchoalveolar lavage fluid
CEES	2-chloroethyl ethyl sulfide
FX	factor X
PAI-1	plasminogen activator inhibitor-1
SM	sulfur mustard
TAT	thrombin-antithrombin complex
TF	tissue factor
TFPI	tissue factor pathway inhibitor

Highlights

- TFPI administration to rats after mustard inhalation reduces airway cast formation.
- Inhibition of thrombin activation is the likely mechanism for limiting casts.
- Rats given TFPI had improved tissue oxygenation, and mortality was prevented.

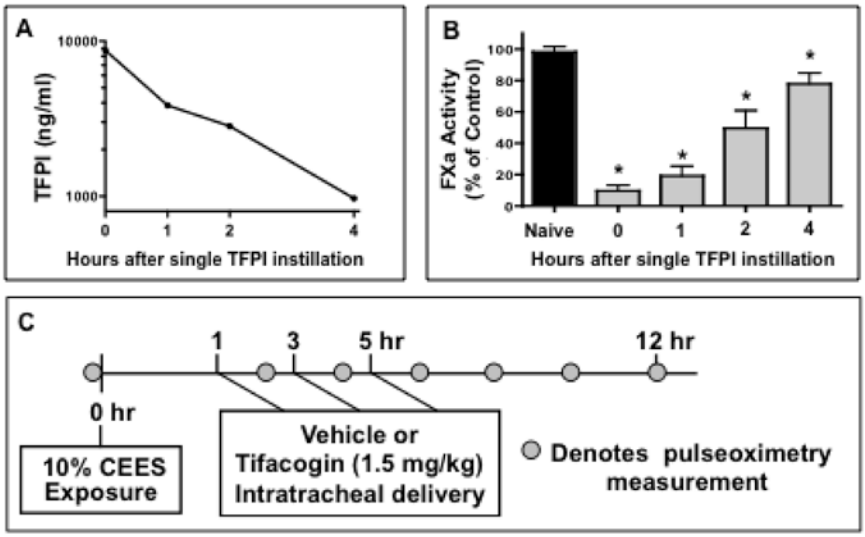

Figure 1. The pharmacokinetics and experimental design of TFPI administration into the rat airway

(A) Measurement of TFPI concentration and rate of elimination from airway surface liquid. TFPI (1.5 mg/kg) was delivered by intratracheal administration, followed by BALF recovery at 0, 1, 2, or 4 hr. Concentrations in these samples, or from naïve rat BALF were determined by ELISA measurement. Each data point represents the mean concentration from three distinct rat subjects. (B) TFPI in BALF demonstrates a time-dependent capacity to inhibit FX to FXa conversion. BALF was incubated with FX, FVII, TF, and Ca^{2+} for 1 hour, and FXa generation determined by measuring chromogenic substrate cleavage. BALF from naïve rats (black bar) had no impact on FXa generation and was assigned an arbitrary value of 100% activity. *$p<0.05$ compared with BALF from the naïve untreated animals. (C) Timeline for use of TFPI as a potential rescue agent in response to inhalation of the mustard analog (CEES). Vehicle only, or vehicle containing TFPI (1.5 mg/kg), was delivered by intratracheal administration in 50 μl volumes at 1, 3 and 5 hours after CEES. Circles on time line denote periodic pulse oximetry measurements.

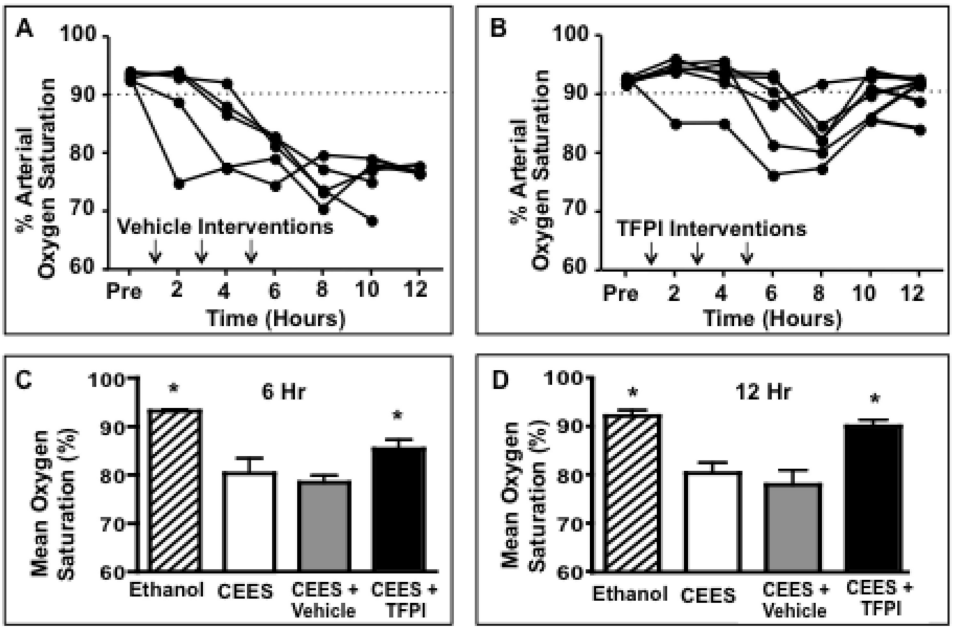

Figure 2. TFPI administration to the airway limits CEES-induced hypoxemia

Panels A & B depict temporal change in arterial oxygen saturation of rats exposed to CEES + vehicle or TFPI. A line failing to extend to the 12 Hr time point indicates mortality, while dotted horizontal lines demarcate the hypoxemic threshold. (C & D) Mean peripheral arterial oxygen saturation values ± SEM at 6 and 12 hr in rats exposed to ethanol control, CEES only, CEES + vehicle, or CEES + TFPI. *p <0.05 compared with mean oxygen saturation of CEES only (white bar) group.

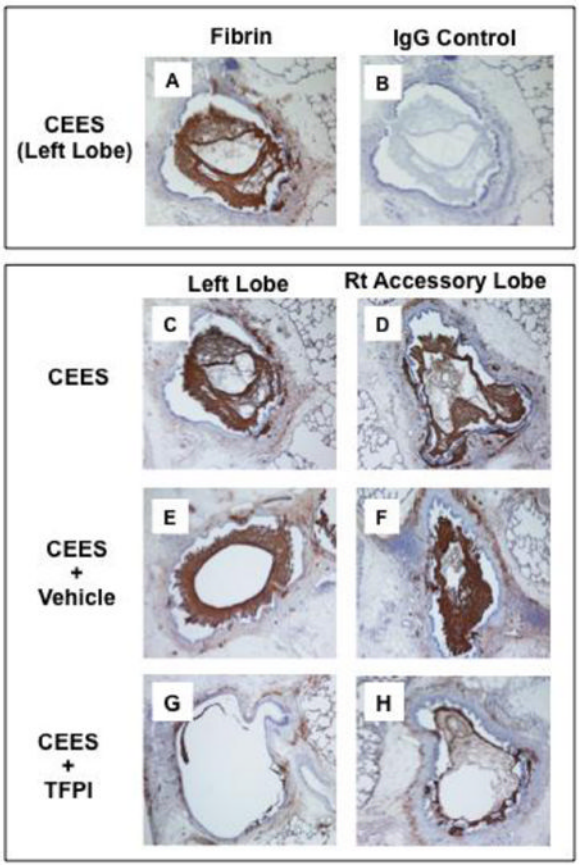

Figure 3. Immunohistochemical detection of intraluminal fibrin deposition on rat lung

Comparison of fibrin (A) and IgG control (B) staining on serial sections of the left lobe obtained 12 hr after 10% CEES exposure. Fibrin staining of primary bronchus in left and right accessory lobe sections after exposure to either: 10% CEES (C, D); 10% CEES + vehicle treatment (E, F); or 10% CEES + TFPI (G, H). Intense fibrin staining is a prominent feature in the major bronchi of both lobes in response to CEES, or CEES + vehicle, whereas staining is greatly reduced at these sites in rats given TFPI.

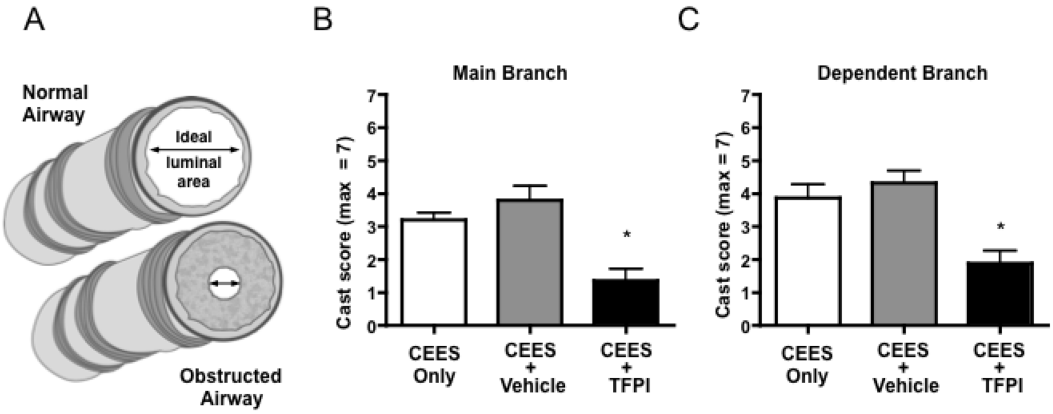

Figure 4. Airway obstruction in response to CEES inhalation and its correction by TFPI administration

(A) Diagram depicting the cross-sectional appearance of a large airway, under normal and obstructed conditions. (B, C) Airway microdissection was used to assess the degree of airway obstruction of rats after exposure to: CEES only; CEES + vehicle; or CEES + TFPI. Panel B presents the mean cast size measurements ± SEM for main lobar bronchi of the left lobe(s). Panel C shows mean cast size measurements of dependent branches of lobes(s). *$p<0.05$ and denotes significant difference in cast size when compared to rats exposed to CEES only (white bar). N= 8 per group.

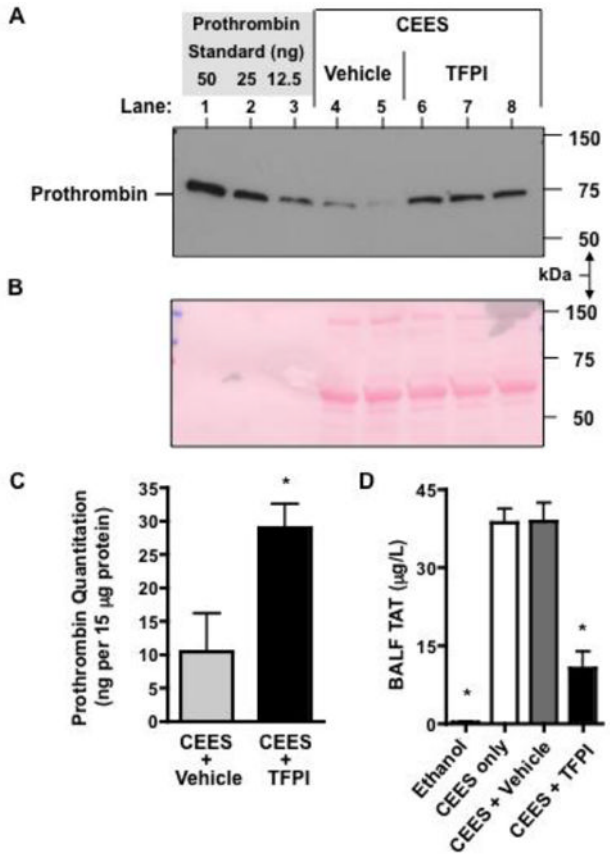

Figure 5. Effects of vehicle or TFPI rescue treatments on prothrombin and thrombin-antithrombin (TAT) levels in rat BALF after CEES inhalation

(A) Western analysis of prothrombin levels. Lanes 1-3 contain rat prothrombin standards (50 - 12.5 ng), lanes 4 & 5 contain rat BALF obtained following CEES + vehicle administration, lanes 6-8 contain rat BALF following CEES + TFPI administration. (B) Ponceau S staining of the PVDF membrane is shown to demonstrate equal protein loading of BALF samples in lanes 4-8. (C) Quantitative comparison of prothrombin levels in BALF. Prothrombin levels were compared between CEES + vehicle (N = 4) and CEES + TFPI (N =6) groups by measurement of band intensities from 2 independent western experiments. *$p<0.05$ and denotes significant difference between the two treatment groups. (D) TAT complex levels in BALF from rats exposed to: ethanol only; CEES only; CEES + vehicle; or CEES + TFPI treatment. Data represents the mean level ± SEM of 4-6 rats. *$p<0.05$ compared with CEES only group.

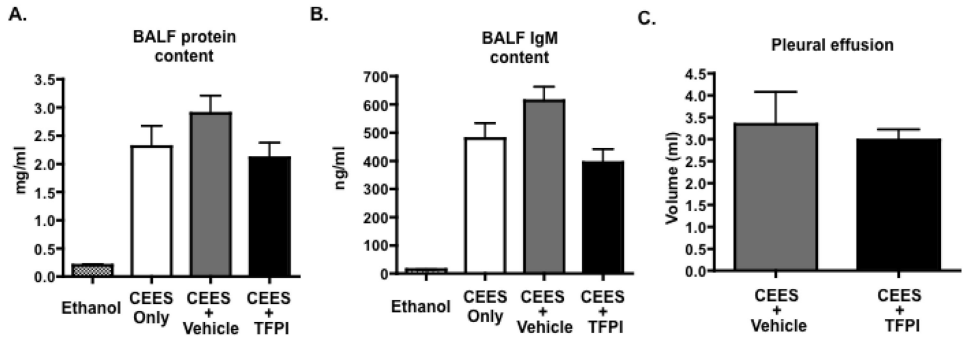

Figure 6. Effect of TFPI administration on CEES-induced airway leak

Lung permeability was assessed in rats administered ethanol, CEES only, CEES + vehicle or CEES + TFPI using several biomarkers: (A) Total protein concentration of BALF; (B) Quantification of IgM levels in BALF by use of a rat IgM ELISA kit; (C) Measurement of fluid accumulation within the pleural cavity. Increased levels of BALF total protein and IgM are consistent with the development of pulmonary vascular leak. Error bars represent SEM. Group comparisons (N =8) were analyzed by one-way ANOVA with Dunnett post hoc test and revealed no significant difference between vehicle and TFPI groups.

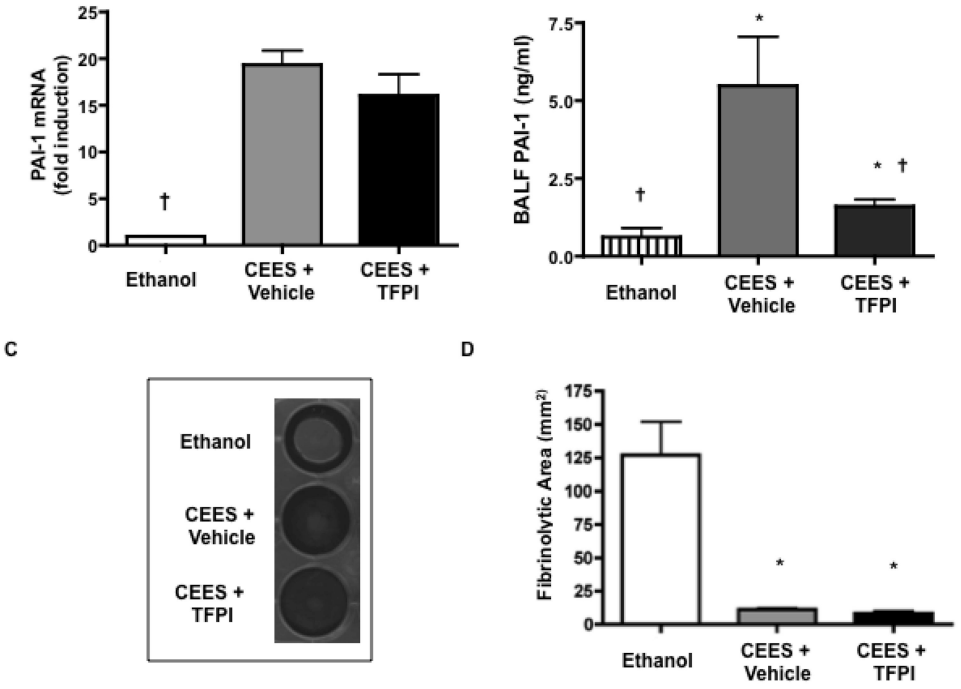

Figure 7. Effect of TFPI administration on CEES-induced PAI-1 expression and fibrinolytic activity of the lung

(A) Lung PAI-1 levels were measured by RT-PCR at 12 Hr after CEES inhalation. Values from ethanol exposed group (white bar) were normalized to one and used to determine the relative fold induction of mRNA in rats receiving CEES + vehicle (grey bar) or CEES + TFPI (black bar). † P<0.05 compared to corresponding CEES + vehicle fraction. (B) Determination of active PAI-1 protein level in BALF as determined by ELISA measurement. * P<0.05 compared to corresponding ethanol control fraction; † P<0.05 compared to CEES + vehicle group. (C) Fibrin plate assay for determining BALF fibrinolytic activity. BALF procedure was performed on rats 12 hr after exposure to ethanol, CEES + vehicle, or CEES + TFPI. After centrifugation, 25 μL of each sample was incubated on a fibrin matrix surface, and stained with buffalo black to distinguish fibrin-containing (black) and hydrolyzed regions (clear). (D) Bars represent the mean fibrinolytic area (clear) ± SD in mm^2 for each treatment condition as determined by NIH image software. (N =4 per group). Each error bars represent SEM. *$P < 0.05$ compared with BALF from ethanol treated rats.

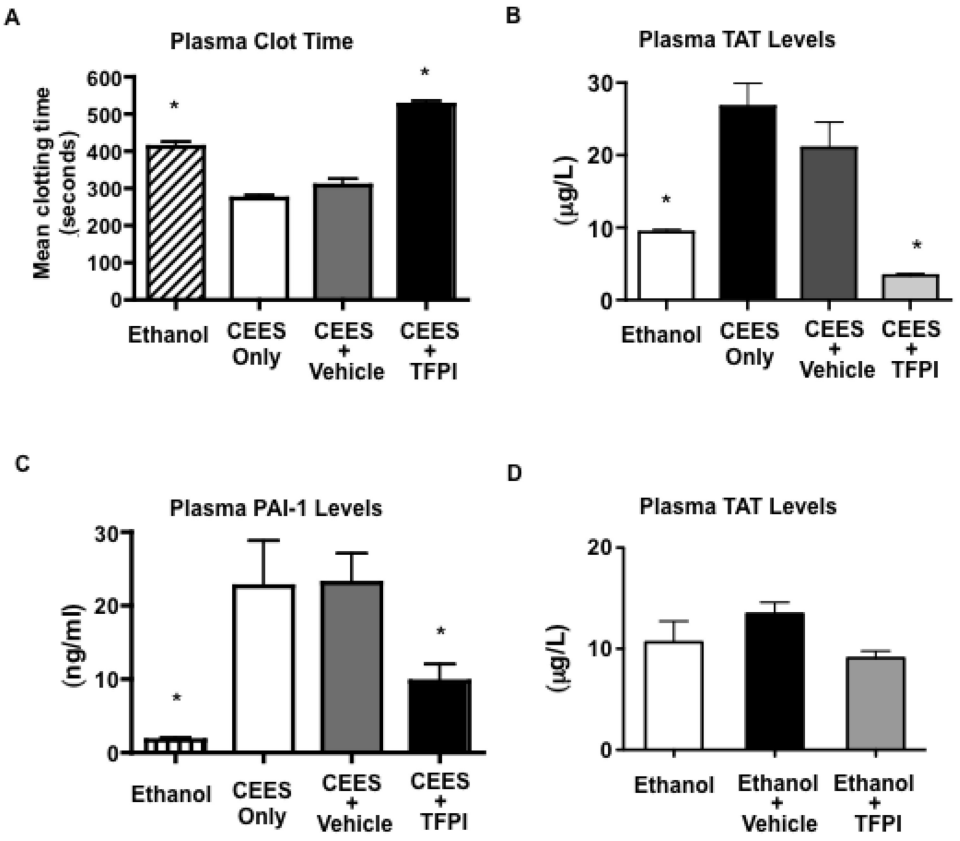

Figure 8. Airway administration of TFPI corrects systemic hypercoagulability and limits mortality in response to CEES inhalation

(A) Platelet poor plasma was prepared from rats exposed to ethanol, CEES only, CEES + vehicle, or CEES + TFPI, using centrifugation and sodium citrate. Clotting times were determined after addition of $CaCl_2$ and spectrophotometric measurement of time-dependent absorbance increase. Bars represent mean clotting time in seconds ± SEM for each treatment condition. *$p<0.05$ and denotes significant difference from CEES only (white bar). Mean concentrations of TAT complex (B) and PAI-1 (C) protein levels in plasma (N = 6 per group). (D) Mean concentration of TAT complex obtained 12 hr after exposure to ethanol, ethanol + vehicle, or ethanol + TFPI (N = 4 per group).

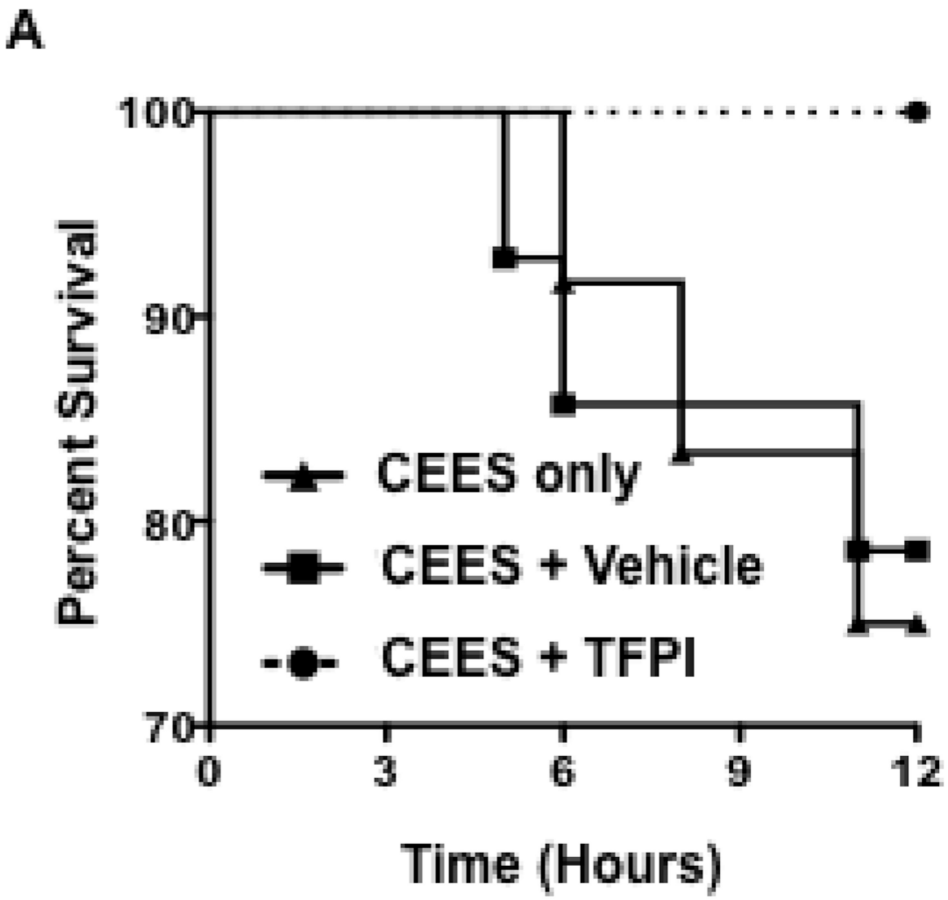

Figure 9. TFPI prevents mortality due to CEES inhalation

Rates of survival in rats after 10% CEES exposure and intratracheal delivery of one of the following treatments: CEES treatment (▲); or CEES + vehicle (■), or CEES + TFPI (dotted line & ●). N = 12, 14, or 16 respectively. Error bars in each graph represent SEM.

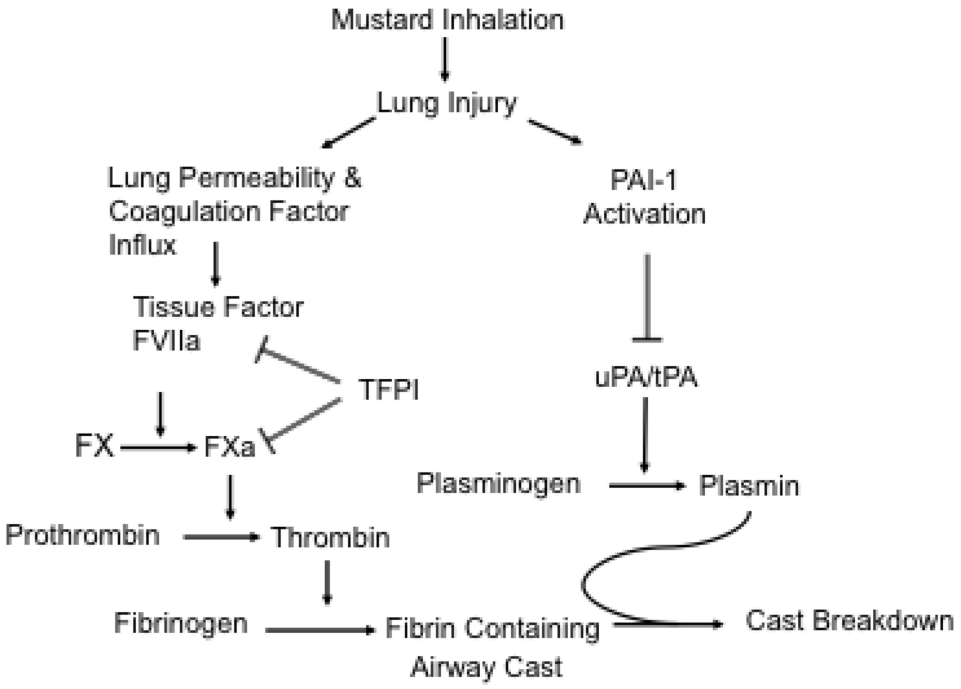

Figure 10. Mechanism for airway cast formation in response to CEES and rationale for TFPI as a rescue therapy

Sulfur mustard inhalation causes injury and subsequent permeability of airways to blood-derived coagulation factors. Activation of the coagulation cascade occurs when extravascular TF present in airways binds FVII, converting it to FVIIa, followed by conversion of FX to active FXa. Factor Xa catalyzes the activation of prothrombin to thrombin, which in turn converts fibrinogen to fibrin. Excessive fibrin deposition causes airway occlusion by forming obstructive casts. TFPI is a serine protease inhibitor capable of binding active sites on both TF/FVIIa complex and FXa. By these inhibitory interactions, TFPI functions as the endogenous regulator of the TF-dependent coagulation. However, TFPI levels are insufficient to prevent airway coagulation during acute lung injury. Airway casts are removed by the fibrinolytic action of plasmin. PAI-1 is elevated in response to acute lung injury and blocks fibrinolysis by inhibiting the plasminogen activators uPA and tPA. This allows nascent airway casts to increase in size.